

# Finite-temperature conductance signatures of quantum criticality in double quantum dots

Luis G. G. V. Dias da Silva,<sup>1,2</sup> Kevin Ingersent,<sup>3</sup> Nancy Sandler,<sup>1</sup> and Sergio E. Ulloa<sup>1</sup>

<sup>1</sup>*Department of Physics and Astronomy and Nanoscale and Quantum Phenomena Institute, Ohio University, Athens, Ohio 45701-2979*

<sup>2</sup>*Materials Science and Technology Division, Oak Ridge National Laboratory, Oak Ridge, TN 37831, and Department of Physics and Astronomy, University of Tennessee, Knoxville, TN 37996*

<sup>3</sup>*Department of Physics, University of Florida, P.O. Box 118440, Gainesville, Florida, 32611-8440*

(Dated: October 31, 2018)

We study the linear conductance through a double-quantum-dot system consisting of an interacting dot in its Kondo regime and an effectively noninteracting dot, connected in parallel to metallic leads. Signatures in the zero-bias conductance at temperatures  $T > 0$  mark a pair of quantum ( $T = 0$ ) phase transitions between a Kondo-screened many-body ground state and non-Kondo ground states. Notably, the conductance features become more prominent with increasing  $T$ , which enhances the experimental prospects for accessing the quantum-critical region through tuning of gate voltages in a single device.

PACS numbers: 73.63.Kv, 73.43.Nq, 72.15.Qm

Quantum phase transitions (QPTs) occur in the zero temperature ( $T = 0$ ) phase diagram of a system at points of nonanalyticity of the ground-state energy.<sup>1,2</sup> QPTs underlie many fascinating phenomena in strongly interacting condensed matter, including the metal-insulator transition in disordered systems,<sup>3</sup> the destruction of antiferromagnetism with doping in high-temperature superconductor parent compounds,<sup>4</sup> the magnetic-field-driven superconducting-insulator transition in disordered superconductors,<sup>5</sup> and quantum Hall plateau transitions.<sup>6</sup> Study of most of these QPTs is hindered by the need to fabricate controlled series of samples at different stoichiometries and/or disorder levels.

By contrast, it is increasingly apparent that systems of quantum dots offer possibilities for exploring QPTs (strictly, *boundary* QPTs involving only a subset of the system degrees of freedom) within a single sample. Advances in system fabrication, precise characterization, and the near suppression of dissipative and incoherent environments<sup>7</sup> have enabled beautiful experiments on multi-dot devices.<sup>8</sup> This leap forward in experimental capability has also spurred much theoretical activity, including several predictions of QPTs in quantum dots in the Kondo regime.<sup>9</sup> The feasibility of realizing nontrivial many-body states has been confirmed by the recent experimental demonstrations of a two-channel Kondo regime<sup>10</sup> and of a singlet-triplet QPT.<sup>11</sup>

This Letter predicts robust signatures of QPTs in the finite-temperature conductance through a double-quantum-dot (DQD) system. A smaller dot (“dot 1”) exhibits Kondo physics, while a larger dot (“dot 2”) is effectively noninteracting and lies near a transmission resonance. When the dots are connected in parallel to external leads, and the system is fine-tuned via applied voltages that determine tunneling barriers and the energies of individual dot orbitals, a *pseudogap* in the low-energy effective hybridization between dot 1 and the leads gives rise to a pair of continuous QPTs between Kondo-

screened and non-Kondo ground states.<sup>12</sup> We describe how the system can be steered into the vicinity of a QPT by monitoring the linear conductance while changing just two gate voltages.

Experimental detection of QPTs necessarily relies on finite-temperature manifestations of the underlying  $T = 0$  transition. We show that the signatures of quantum criticality in the present DQD system become more pronounced as the temperature is increased from absolute zero, a trend that contrasts with the typical behavior near an impurity QPT.<sup>2</sup> Their temperature dependence also allows these signatures to be distinguished from other conductance features in the same system.

*Model and conductance calculation.*—Consider a DQD device in which dot 1 is in an odd-electron-number Coulomb blockade valley, and dot 2 has a single level near the Fermi level and is effectively noninteracting.<sup>13</sup> The dots are coupled to left ( $L$ ) and right ( $R$ ) metallic leads and to each other via tunneling barriers. This device is described by a two-impurity Anderson Hamiltonian:

$$H = \sum_{i,\sigma} \varepsilon_i n_{i\sigma} + U_1 n_{1\uparrow} n_{1\downarrow} + \sum_{\sigma} \left( \lambda a_{1\sigma}^\dagger a_{2\sigma} + \text{H.c.} \right) + \sum_{\ell,\mathbf{k},\sigma} \varepsilon_{\ell\mathbf{k}} c_{\ell\mathbf{k}\sigma}^\dagger c_{\ell\mathbf{k}\sigma} + \sum_{i,\ell,\mathbf{k},\sigma} \left( V_{i\ell} a_{i\sigma}^\dagger c_{\ell\mathbf{k}\sigma} + \text{H.c.} \right), \quad (1)$$

where  $a_{i\sigma}^\dagger$  creates a spin- $\sigma$  electron in dot  $i$  ( $= 1, 2$ ),  $n_{i\sigma} = a_{i\sigma}^\dagger a_{i\sigma}$ , and  $c_{\ell\mathbf{k}\sigma}^\dagger$  creates a spin- $\sigma$  electron of wave vector  $\mathbf{k}$  and energy  $\varepsilon_{\ell\mathbf{k}}$  in lead  $\ell$  ( $= L, R$ ). We assume for simplicity that each lead has a density of states  $\rho(\omega) = \rho_0 \Theta(D - |\omega|)$ , symmetric about the Fermi energy ( $\omega = 0$ ), and that dot-lead couplings are local. We further assume that all couplings are real and the device is tuned to left-right symmetry, so that we can write  $V_{i\ell} = V_i / \sqrt{2}$ .

The linear conductance at temperature  $T$  for this DQD

setup can be obtained from the Landauer formula as:

$$g(T) = g_0 \int_{-\infty}^{\infty} d\omega (-\partial f/\partial\omega) [-\text{Im} \mathcal{T}(\omega)], \quad (2)$$

$$\mathcal{T}(\omega) = 2\pi\rho_0 \sum_{i,j} V_{iL}^* G_{ij}(\omega) V_{jR}, \quad (3)$$

where  $g_0 = 2e^2/h$ ,  $f(\omega/T) = [\exp(\omega/T) + 1]^{-1}$  is the Fermi-Dirac function, and all  $G_{ij}(\omega)$  in Eq. (3) are dressed Green's functions, fully taking into account the electron-electron interactions on dot 1.

The standard equations of motion  $\omega \langle\langle A; B \rangle\rangle_{\omega} - \langle\{A, B\}\rangle = \langle\langle [A, H]; B \rangle\rangle_{\omega} = -\langle\langle A; [B, H] \rangle\rangle_{\omega}$  for the retarded Green's function  $\langle\langle A; B \rangle\rangle_{\omega} = -i \int_0^{\infty} dt e^{i\omega t} \langle\{A(t), B(0)\}\rangle$  allow one to re-express  $G_{ij}(\omega) = \langle\langle a_{i\sigma}; a_{j\sigma}^{\dagger} \rangle\rangle_{\omega}$  in terms of  $G_{11}$  and the bare Green's function  $G_{22}^{(0)}$ , which describes the noninteracting dot 2 in the absence of dot 1. In the wide-band limit  $|\omega| \ll D$ ,<sup>13</sup> Eq. (3) becomes

$$\begin{aligned} \mathcal{T}(\omega) = & \Delta_1 G_{11}(\omega) + 2\Delta_{12} [G_{22}^{(0)}(\omega) (\lambda - i\Delta_{12}) G_{11}(\omega)] \\ & + \Delta_2 [1 + G_{22}^{(0)}(\omega) (\lambda - i\Delta_{12})^2 G_{11}(\omega)] G_{22}^{(0)}(\omega), \end{aligned} \quad (4)$$

where  $\Delta_i = \pi\rho_0 V_i^2$ ,  $\Delta_{12} = \pi\rho_0 V_1 V_2$ , and  $G_{22}^{(0)}(\omega) = (\omega - \varepsilon_2 + i\Delta_2)^{-1}$ .

The dot-1 local Green's function  $G_{11}(\omega)$  entering Eq. (4) can be obtained<sup>12</sup> by mapping the Hamiltonian (1) to an effective model of a single dot connected to the leads via a nonconstant hybridization function

$$\Delta(\omega) = \pi\rho_2(\omega) \left[ \lambda + (\omega - \varepsilon_2) \sqrt{\Delta_1/\Delta_2} \right]^2, \quad (5)$$

with  $\rho_2(\omega) = \Delta_2 / \{\pi[(\omega - \varepsilon_2)^2 + \Delta_2^2]\}$ . We solve this effective model using the numerical renormalization group.<sup>14</sup> At  $T > 0$ , we compute the spectral function  $A_{11}(\omega) = -\pi^{-1} \text{Im} G_{11}(\omega)$ , and hence obtain  $G'_{11}(\omega) = \text{Re} G_{11}(\omega)$  via a Kramers-Kronig transformation. At  $T = 0$ , where Eq. (2) involves only  $G_{11}(0)$ , it is possible to calculate  $G'_{11}(0)$  directly. All results shown are for  $U_1 = 0.5D$  and  $\Delta_2 = 0.02D$  with temperatures in units of  $T_{K0} = 7.0 \times 10^{-4}D$ , the Kondo temperature in the reference case where dot 2 is decoupled ( $\lambda = \Delta_2 = 0$ ) and  $U_1 = -2\varepsilon_1 = 0.5D$ ,  $\Delta_1 = 0.05D$ .

To facilitate interpretation of the results, we note that  $-\text{Im} \mathcal{T}(\omega)$  entering Eq. (2) can be expressed as

$$\begin{aligned} -\text{Im} \mathcal{T}(\omega) = & [1 - 2\pi\Delta_2\rho_2(\omega)] \pi\Delta(\omega)A_{11}(\omega) + \pi\Delta_2\rho_2(\omega) \\ & + 2\pi(\omega - \varepsilon_2)\Delta(\omega)\rho_2(\omega)G'_{11}(\omega). \end{aligned} \quad (6)$$

The term  $\pi\Delta_2\rho_2(\omega)$  represents bare transmission through dot 2 in the absence of dot 1, and for  $T \ll \Delta_2$  yields a conductance contribution  $g_2 \simeq g_0\Delta_2^2/(\varepsilon_2^2 + \Delta_2^2)$ . In most cases of interest, the term involving  $G'_{11}$  turns out to be negligible. If, as we assume, the dot-1 level is off resonance (i.e.,  $|\varepsilon_1| \gg T, \Delta_1$ ), then dot 1 appreciably influences  $g$  only in the Kondo regime  $T \lesssim T_K$  where  $A_{11}(\omega)$  exhibits a many-body resonance at the Fermi level; the

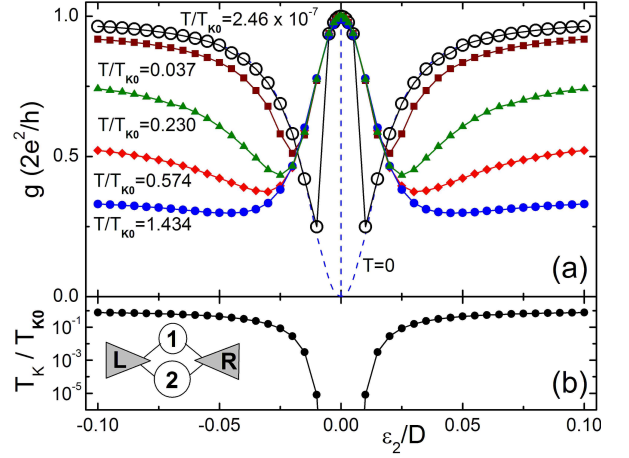


FIG. 1: (color online) (a) Conductance  $g$  vs  $\varepsilon_2$  at six temperatures for a *parallel* DQD device [inset in (b)] with  $\varepsilon_1 = -U_1/2$  and  $\Delta_1 = 0.05D$ . (b) Transmission through dot 1 sets in below the Kondo temperature  $T_K$  (defined as in 12), which vanishes as  $\varepsilon_2 \rightarrow 0$ .

sign of the resulting conductance term  $g_1$  depends on that of  $1 - 2\pi\Delta_2\rho_2(\omega)$  in the range  $|\omega| \lesssim O(T)$  that determines  $g(T)$ . For  $|\varepsilon_2| \gg \Delta_2$  ( $|\varepsilon_2| \ll \Delta_2$ ),  $g_1$  is positive (negative) at low temperatures, leading to constructive (destructive) interference with  $g_2$ .

*Tuning to the pseudogap regime.*—When the level energy in dot 2 is set to  $\varepsilon_2 = \lambda\sqrt{\Delta_2/\Delta_1}$ , the dot-1 effective hybridization [Eq. (5)] vanishes at the Fermi level as  $\Delta(\omega) \propto \omega^2$ . The pseudogap Anderson impurity model, in which  $\Delta(\omega) \propto |\omega|^r$  for  $|\omega| \rightarrow 0$ , exhibits Kondo and non-Kondo ground states separated by QPTs. Whereas previous theoretical work<sup>15</sup> has focused on exponents  $0 < r \leq 1$ , the proposed DQD setup offers a controlled realization of the case  $r = 2$ , which features a pair of QPTs. For simplicity, we focus in the remainder of the paper on configurations in which the dots are connected to the leads purely in parallel, i.e.,  $\lambda = 0$  [see inset in Fig. 1(b)]. Then Eq. (5) reduces to  $\Delta(\omega) = \Delta_1(\omega - \varepsilon_2)^2/[(\omega - \varepsilon_2)^2 + \Delta_2^2]$ .

In order to probe the QPTs, the pseudogap in  $\Delta(\omega)$  must be centered on the Fermi energy. Operationally, this can be accomplished by tuning  $\varepsilon_2$  (via a plunger gate voltage on dot 2) to reach a maximum of  $g$ . Figure 1(a) illustrates  $g$  vs  $\varepsilon_2$  at six temperatures, for fixed  $\varepsilon_1 = -U_1/2$  and  $\Delta_1 = 0.05D$ . For  $\lambda = 0$ ,  $\Delta(0) = 0$  when dot 2 is exactly in resonance with the leads:  $\varepsilon_2 = 0$ . The choice of  $\varepsilon_1 = -U_1/2$  makes  $\varepsilon_2 = 0$  a point of particle-hole (p-h) symmetry, and ensures that for  $|\varepsilon_2| \ll \Delta_2$  and  $T \ll T_K$ ,  $\pi\Delta(0)A_{11}(0) \simeq 1$ ;<sup>16</sup> then, since  $\pi\Delta_2\rho_2(0) \simeq 1$ ,  $g_1$  almost completely cancels  $g_2$ . Figure 1(b) shows that the temperature range  $0 \leq T \lesssim T_K(\varepsilon_2)$  of the low-conductance regime shrinks rapidly as  $\varepsilon_2 \rightarrow 0$ . For the special case  $\varepsilon_2 = 0$ , the pseudogap in  $\Delta(\omega)$  prevents the formation of a Kondo state (effectively,  $T_K = 0$ ), and transport takes place solely through dot 2. At  $T = 0$ , the resulting conductance exhibits a discrete jump from

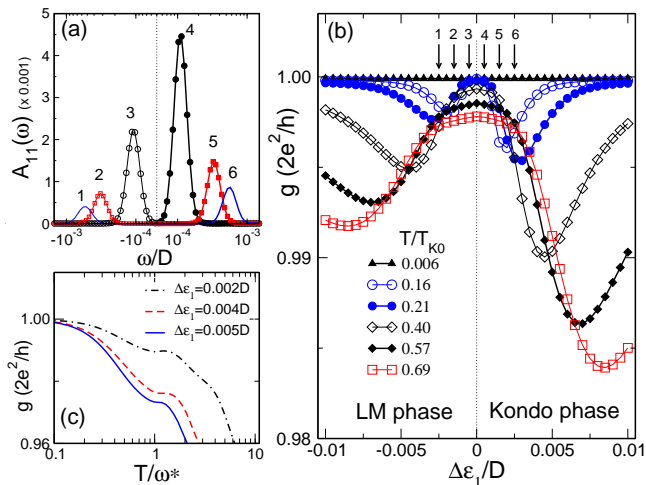


FIG. 2: (color online) Behavior near the  $\varepsilon_{1c}^+$  transition in a parallel DQD device with  $\Delta_1 = 0.05D$  and  $\varepsilon_2 = 0$ : (a) Curves 1–6 show the dot-1 spectral function  $A_{11}(\omega)$  for the values of  $\Delta\varepsilon_1 = \varepsilon_1 - \varepsilon_{1c}^+$  indicated by the corresponding arrows in (b). The frequency  $\omega^*$  of the quasiparticle peak in  $A_{11}(\omega)$  is proportional to  $\Delta\varepsilon_1$ . (b) Conductance  $g$  vs  $\Delta\varepsilon_1$  at six temperatures. (c)  $g$  vs  $T/\omega^*$  at three values of  $\Delta\varepsilon_1$  on the Kondo side of the transition.

$g = 0$  for  $|\varepsilon_2| \rightarrow 0$  to  $g = g_0$  for  $\varepsilon_2 = 0$  [dashed line in Fig. 1(a)]. However, this spike broadens at  $T > 0$  into a smooth peak rising to  $g(\varepsilon_2 = 0) \simeq g_0$ .

For a general  $\varepsilon_1 \neq -U_1/2$ , transmission through dot 1 is still blocked when  $\Delta(0) = 0$ . This leads to an asymmetric peak in  $g(\varepsilon_2)$  at  $g(0) \simeq g_0$ —a feature that again broadens with increasing  $T$ ,<sup>17</sup> offering a practical method for tuning the pseudogap to the Fermi level.

*Tuning to a QPT.*—With  $\varepsilon_2$  held at zero, the level energy  $\varepsilon_1$  can be varied via a plunger gate voltage on dot 1. A pair of QPTs, related by p-h duality and located at  $\varepsilon_1 = \varepsilon_{1c}^\pm = -U_1/2 \pm |\Delta\varepsilon_{1c}|$ , bound a local-moment (LM) regime  $\varepsilon_{1c}^- < \varepsilon_1 < \varepsilon_{1c}^+$  in which the net spin on dot 1 is unscreened at  $T = 0$ . Close to either QPT,  $A_{11}(\omega)$  contains a quasiparticle peak centered at  $\omega = \omega^*$ , where  $\omega^* \propto \varepsilon_1 - \varepsilon_{1c}^\pm$  [Fig. 2(a)]. The peak sets in below a crossover temperature  $\simeq |\omega^*|$ , which on the Kondo side is proportional to  $T_K$ . This feature in  $A_{11}(\omega)$  leads, via Eqs. (2) and (6), to a conductance contribution  $g_1 < 0$  that is greatest in magnitude when  $|\omega^*| \simeq 4T$ . Since the dot-2 contribution  $g_2 \simeq g_0$  is independent of  $\varepsilon_1$ ,  $g$  vs  $\varepsilon_1$  isotherms [e.g., see Fig. 2(b)] show a dip at  $|\varepsilon_1 - \varepsilon_{1c}^\pm| \propto T$  on either side of a maximum at  $\varepsilon_1 = \varepsilon_{1c}^\pm$ .

It is striking that at  $T = 0$ , the conductance shows no feature as dot 1 passes through a QPT. At finite temperatures, by contrast, the DQD device can be tuned to the transition by seeking a local maximum in  $g$  vs  $\varepsilon_1$ . This maximum has the identifying characteristics [Fig. 2(b)] that the minima on either side are equidistant in  $\varepsilon_1$  from  $\varepsilon_{1c}^\pm$ , but the dip in  $g$  is roughly twice as deep on the Kondo side, reflecting the greater weight of the quasiparticle peak in that regime. For the parameters shown in Fig. 2(b), the conductance peak becomes more

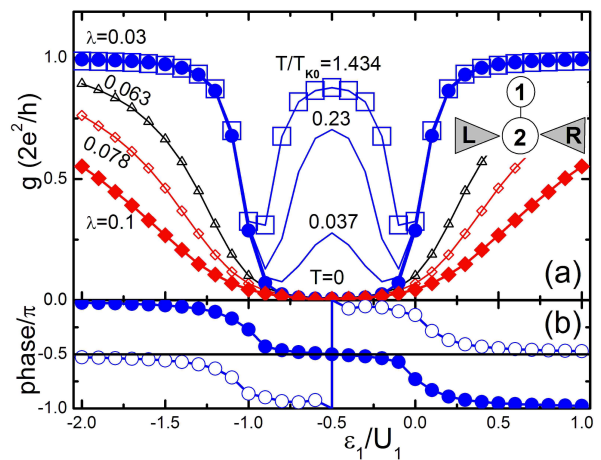


FIG. 3: (color online) (a) Conductance  $g$  vs  $\varepsilon_1$  for a *side-dot* device (inset) with  $\varepsilon_2 = 0$ , both for  $T = 0$  at various  $\lambda$  values and for  $\lambda = 0.03D$  at the labeled temperatures. (b) Phase shifts  $\eta_{11}$  (filled circles) and  $\eta_{22}$  (open circles) for  $\lambda = 0.03D$ ,  $T = 0$ ;  $g$  vanishes when  $\sin \eta_{22} = 0$  [Eq. (7)].

prominent with increasing temperature up to  $T \simeq 3T_{K0}$ , and a peak in  $g$  remains discernible up to the relatively high scale  $T \simeq 6T_{K0}$ .

The form of  $g$  vs  $T$  at fixed  $\varepsilon_1$  is more complicated since  $g_1$  and  $g_2$  can have temperature variations of comparable magnitude. Figure 2(c) shows that in the Kondo regime, the peak in  $|g_1(T)|$  contributes a shoulder around  $T = |\omega^*|$  to the overall downward trend dictated by  $g_2(T)$ . Similar behavior holds in the LM regime (not shown).

*Differentiating QPT and other conductance features.*—Conductance peaks similar to those shown in Fig. 2(b) can also arise, not from proximity to a QPT, but rather from interference between a conventional (metallic or  $r = 0$ ) many-body Kondo resonance on dot 1 and a noninteracting resonance on dot 2. In experiments, the mapping between the gate voltages in a real device and parameters of the effective Anderson model will not be known *a priori*. It is therefore important to be able to identify unique signatures of a QPT in this system. We show below that the temperature dependence of the conductance peaks serves this purpose.

For simplicity, we consider the “side-dot” regime<sup>18</sup>  $\Delta_1 = 0$  in which dot 1 is connected to the leads only via the noninteracting dot 2. In this geometry [inset in Fig. 3(a)], the effective dot-1 hybridization function  $\Delta(\omega) = \pi\lambda^2\rho_2(\omega)$  [from Eq. (5)] is a Lorentzian of width  $\Delta_2$  centered at  $\omega = \varepsilon_2$ . Since  $\Delta(\omega)$  has no pseudogap, there is no QPT.

Figure 3 plots the variation of the conductance with the position  $\varepsilon_1$  of the energy level in the side dot 1 while dot 2 is held in resonance, i.e.,  $\varepsilon_2 = 0$ . At  $T = 0$ , the conductance drops to zero as  $\varepsilon_1$  approaches the p-h-symmetric point  $\varepsilon_1 = -U/2$ , independent of the dot-dot coupling  $\lambda$ . This can be understood by noting that for

$\Delta_1 = 0$  and  $T = 0$ , Eqs. (2) and (3) reduce to

$$g(T = 0) = -g_0 \Delta_2 |G_{22}(0)| \sin \eta_{22}, \quad (7)$$

where  $\eta_{ii} = \arg G_{ii}(0)$  is the Fermi-energy phase shift of electrons scattering from dot  $i$ . Figure 3(b) shows that in a window about the p-h-symmetric point, the dot-1 phase shift exhibits a plateau  $\eta_{11} \simeq -\pi/2$  characteristic of the Kondo state.<sup>19</sup> This additional phase shift of electrons that scatter from the side dot on their path between the two leads renormalizes the bare dot-2 phase shift  $\eta_{22}^{(0)} = -\pi/2$  to produce an  $\eta_{22}$  that jumps from  $-\pi$  to 0 at the p-h point. On moving away from  $\varepsilon_1 = -U_1/2$ , dot 1 gradually enters its mixed-valence regime, where there is no Kondo resonance and the  $T = 0$  conductance rises towards its unitary limit  $g = g_0$ . With increasing  $\lambda$ , the Kondo state in dot 1 becomes more robust (as evidenced<sup>12</sup> by its larger  $T_K$ ), pushing this upturn in  $g$  to larger values of  $|\varepsilon_1 + U_1/2|$ .

Raising the temperature progressively destroys the Kondo resonance and thereby increases the conductance. For fixed  $T > 0$ ,  $g$  vs  $\varepsilon_1$  reaches a peak at  $\varepsilon_1 = -U_1/2$ , where  $T_K$  is smallest and Kondo scattering is weakest. Figure 3(a) illustrates this behavior at three temperatures for  $\varepsilon_2 = 0$ ,  $\lambda = 0.03D$ . The double-dip structure surrounding the peak in  $g$  vs  $\varepsilon_1$  is qualitatively similar to

the QPT feature in Fig. 2(b). However, the temperature variation is very different in the two cases. In Fig. 2(b), the *decrease* with increasing  $T$  of the conductance both at the peak and at the minima on either side is characteristic of the QPT. By contrast, conductance peaks arising for  $\Delta(0) \neq 0$  exhibit an *increase* with  $T$  of the extremal  $g$  values, as seen in Fig. 3(a).

To conclude, we have studied the linear conductance through a class of quantum-dot devices that can be described by a single Anderson impurity coupled to a conduction band via a nonconstant hybridization function. Such devices can be tuned to a quantum phase transition, marked by a near-unitary peak in the linear conductance that becomes more pronounced with increasing temperatures. The details of its evolution with temperature differentiate this conductance signature from similar features arising from interference effects unrelated to quantum criticality. Our results demonstrate that these quantum-dot devices offer many advantages for the controlled experimental investigation of a rich array of many-body physics.

We thank C. Lewenkopf, C. Büsser, and E. Vernek for valuable discussions, and support under NSF-DMR grants 0312939 and 0710540 (Florida), 0336431, 0304314 and 0710581 (Ohio), and 0706020 (Tennessee).

- 
- <sup>1</sup> S. Sachdev, *Quantum Phase Transitions* (Cambridge University Press, Cambridge, U.K., 1999).  
<sup>2</sup> M. Vojta, *Phil. Mag.* **86**, 1807 (2006).  
<sup>3</sup> A. Husmann *et al.*, *Science* **274**, 1874 (1996).  
<sup>4</sup> S. Sachdev, *Rev. Mod. Phys.* **75**, 913 (2003).  
<sup>5</sup> N. Mason and A. Kapitulnik, *Phys. Rev. Lett.* **82**, 5341 (1999).  
<sup>6</sup> S. L. Sondhi, S. M. Girvin, J. P. Carini, and D. Shahar, *Rev. Mod. Phys.* **69**, 315 (1997).  
<sup>7</sup> D. Goldhaber-Gordon *et al.*, *Nature (London)* **391**, 156 (1998).  
<sup>8</sup> H. Jeong, A. M. Chang, and M. R. Melloch, *Science* **293**, 2221 (2001); N. J. Craig *et al.*, *ibid.* **304**, 565 (2004); J. C. Chen, A. M. Chang, and M. R. Melloch, *Phys. Rev. Lett.* **92**, 176801 (2004); A. Fuhrer, T. Ihn, K. Ensslin, W. Wegscheider, and M. Bichler, *ibid.* **93**, 176803 (2004); R. Leturcq *et al.*, *ibid.* **95**, 126603 (2005).  
<sup>9</sup> W. Hofstetter and H. Schoeller, *Phys. Rev. Lett.* **88**, 016803 (2001); M. Pustilnik, L. Borda, L. I. Glazman, and J. von Delft, *Phys. Rev. B* **69**, 115316 (2004); M. R. Galpin, D. E. Logan, and H. R. Krishnamurthy, *Phys. Rev. Lett.* **94**, 186406 (2005); G. Zarand, C. H. Chung, P. Simon, and M. Vojta, *ibid.* **97**, 166802 (2006); R. Zitko and J. Bonca, *Phys. Rev. B* **76**, 241305(R) (2007).  
<sup>10</sup> R. M. Potok *et al.*, *Nature (London)* **446**, 167 (2007).  
<sup>11</sup> N. Roch *et al.*, *Nature* **453**, 633 (2008).  
<sup>12</sup> (a) L. G. G. V. Dias da Silva, N. P. Sandler, K. Ingersent, and S. E. Ulloa, *Phys. Rev. Lett.* **97**, 096603 (2006); (b) *ibid.* **99**, 209702 (2007).

- <sup>13</sup> The assumptions of a noninteracting dot 2 and a wide band simplify the analysis, but essentially the same properties arise from the full solution of Eq. (1) for a weakly interacting dot 2, as will be discussed elsewhere.<sup>17</sup>  
<sup>14</sup> R. Bulla, T. A. Costi, and T. Pruschke, *Rev. Mod. Phys.* **80**, 395 (2008).  
<sup>15</sup> D. Withoff and E. Fradkin, *Phys. Rev. Lett.* **64**, 1835 (1990); C. Gonzalez-Buxton and K. Ingersent, *Phys. Rev. B* **54**, R15614 (1996); *ibid.* **57**, 14254 (1998); R. Bulla, Th. Pruschke, and A. C. Hewson, *J. Phys. Condens. Matter* **9**, 10463 (1997); M. Vojta and R. Bulla, *Phys. Rev. B* **65**, 014511 (2001); L. Fritz and M. Vojta, *ibid.* **70**, 214427 (2004).  
<sup>16</sup> L. Vaugier, A. A. Aligia, and A. M. Lobos, *Phys. Rev. Lett.* **99**, 209701 (2007).  
<sup>17</sup> W. B. Lane, K. Ingersent, L. G. G. V. Dias da Silva, N. P. Sandler, and S. E. Ulloa, in preparation.  
<sup>18</sup> K. Kang, S. Y. Cho, J.-J. Kim, and S.C. Shin, *Phys. Rev. B* **63**, 113304 (2001); V. M. Apel *et al.*, *Microelectr. J.* **34**, 729 (2003); C. A. Büsser *et al.*, *Phys. Rev. B* **70**, 245303 (2004); P. S. Cornaglia and D. R. Grempel, *ibid.* **71**, 075305 (2005); P. Simon, J. Salomez, and D. Feinberg, *ibid.* **73**, 205325 (2006); R. Zitko and J. Bonca, *ibid.* **73**, 035332 (2006); P. A. Orellana, G. A. Lara, and E. V. Anda, *ibid.* **74**, 193315 (2006); A. C. Seridonio, M. Yoshida, and L. N. Oliveira, arXiv:cond-mat/0701529 (2007).  
<sup>19</sup> U. Gerland, J. von Delft, T. A. Costi, and Y. Oreg, *Phys. Rev. Lett.* **84**, 3710 (2000).